Safety and Connectivity Certificates for Finite-Time Formation Transitions

Yash Purswani, Shivansh Agarwal and Anuj Tiwari

arXiv:2611.13927v1 [eess.SY] 10 Nov 2026

***Abstract*— Finite-time formation transitions are useful for coordinating multi-agent systems in time-critical missions, but convergence to a prescribed formation in finite time does not guarantee collision avoidance or communication connectivity during the transition. Existing approaches address finite-time coordination and safety-constrained formation control, yet explicit connections between disagreement during transitions, formation geometry, and coupling-gain selection need to be developed for certifying safe maneuvers. This paper develops a disagreement-based framework for certifying transient safety and connectivity during finite-time tracking of arbitrary prescribed formation trajectories. Local feedback guarantees exact finite-time tracking with a graph-independent settling-time bound, while a graph-dependent disagreement bound is used to derive sufficient geometric conditions for collision avoidance and connectivity preservation. These conditions further yield an offline coupling-gain selection rule based on the available geometric clearance. Numerical simulations illustrate the trade-off between convergence rate and control effort as the coupling gain increases. They also demonstrate the effectiveness and conservatism of the proposed certificates.**

***Index Terms*— Distributed cooperative control over networks, Safety critical systems, Stability of nonlinear systems, Formation control.**

I. Introduction

Multi-agent systems enable tasks such as cooperative transportation, autonomous navigation, and distributed sensing, where multiple agents must follow a moving reference while maintaining a prescribed spatial arrangement [1]–[3]. Formation-control frameworks commonly exploit inter-agent interactions and graph-based coordination to achieve desired collective configurations [4], [5]. In practical missions, however, formations may be asymmetric or time-varying, requiring agents to track individually prescribed formation positions as the formation translates, rotates, or deforms.

For time-critical maneuvers, asymptotic convergence may be insufficient, motivating finite-time tracking with an explicit settling bound [6], [7]. During such maneuvers, collision avoidance and communication connectivity must also be maintained as agents move toward their prescribed formation positions. These properties depend on the relative positions of agents, which are influenced by disagreement, i.e., differences in their individual formation tracking errors. This motivates quantifying how the disagreement evolves during finite-time transitions and relating its bounds to collision avoidance and connectivity preservation throughout the maneuver.

This work has been submitted to the IEEE for possible publication. Copyright may be transferred without notice, after which this version may no longer be accessible.

The authors are with the Department of Mechanical Engineering, Indian Institute of Technology Madras, Chennai 600036, India. me22b214@smail.iitm.ac.in, me24s022@smail.iitm.ac.in, anujt@iitm.ac.in

Existing works provide convergence guarantees for finite-time consensus and formation control under varied interaction structures [8], [9]. Fedele and D'Alfonso [10] studied finite-time centroid tracking with bounded aggregation, while collision avoidance and connectivity preservation have been addressed through energy-based, optimization, and barrier-function approaches [11]–[14]. In contrast, this work investigates how cooperative disagreement contraction can provide explicit transient safety and connectivity certificates for individually prescribed formation trajectories, without modifying the nominal tracking protocol or requiring online safety optimization.

This paper considers a distributed first-order kinematic protocol for tracking arbitrary prescribed C^1 formation trajectories. Local feedback guarantees exact finite-time formation tracking with a graph-independent settling-time bound. A graph-dependent analysis shows that the relative tracking errors are bounded, which is then translated into sufficient geometric conditions for pairwise collision avoidance and preservation of a prescribed connected spanning sub-graph. These conditions subsequently lead to an offline design rule for the coupling-gain selection, based on the planned formation geometry and initial disagreement among agents. The protocol generates velocity setpoints for low-level controllers or autopilots, providing a common kinematic framework for coordinating agents with higher order and heterogeneous dynamics. The main contributions of this can be summarized as follows,

1) We propose a distributed first-order kinematic framework that guarantees finite-time formation tracking with a graph-independent settling-time bound for arbitrary prescribed C^1 trajectories.
2) We derive a graph-dependent bound on disagreement that accounts for cooperative coupling under undirected, time-varying communication graphs.
3) We use the disagreement bound to establish sufficient conditions for collision avoidance and connectivity preservation, and derive an offline coupling-gain selection rule based on the planned formation geometry and initial disagreement.

II. Background and Problem Definition

Consider a multi-agent system having $n \geq 2$ agents, with position state $x_i \in \mathbb{R}^d$ in d dimensions, and desired position $x_{d,i}(t)$ for each agent i in a given formation, where,

$$x_{d,i}(t) = r(t) + p_i(t), \qquad \delta_i(t) = x_i(t) - x_{d,i}(t), \quad (1)$$

where $r(t) \in \mathbb{R}^d$ is the reference trajectory of the formation and and $p_i(t) \in \mathbb{R}^d$ is the desired offset relative to this

reference. The prescribed trajectories $x_{d,i}(t)$ are assumed to be continuously differentiable, allowing the formation to translate and deform over time.

The distributed kinematic protocol for the swarm agents can be given as,

$$\dot{x}_i = -\delta_i - \Phi_\beta(\delta_i) - \sum_{j=1}^{n} w_{ij} M(\delta_i - \delta_j) + \dot{x}_{d,i}, \quad (2)$$

where $\dot{x}_i$ is the ideal commanded velocity, $w_{ij} \geq 0$ are interaction weights, and $M \in \mathbb{R}^{d\times d}$ is symmetric positive semi-definite coupling matrix. For $0 < \beta < 1$, the local component-wise fractional-power feedback is

$$[\Phi_\beta(z)]_k = \operatorname{sign}(z_k)|z_k|^\beta, \qquad k = 1, \ldots, d, \quad (3)$$

with $\Phi_\beta(0) = 0$.

In a network of mobile agents, communication is usually limited to nearby agents, and the available links may change as the agents move. We describe the communication network by a time-varying undirected graph $\mathcal{G}(t) = (\mathcal{V}, \mathcal{E}(t))$, where $\mathcal{V} = \{1, \ldots, n\}$ is the set of agents and $\mathcal{E}(t)$ contains the active communication links [15], [16]. Links may be established or lost as inter-agent distances cross the communication range, changing the graph topology while agent state x_i remains continuous.

The inter-agent interaction weights w_{ij} are designed as

$$w_{ij}(x) = \frac{a_{ij}(x)}{\|x_i - x_j\|^\nu + \varepsilon_w}, \qquad \nu \geq 1, \quad \varepsilon_w > 0, \quad (4)$$

where

$$a_{ij}(x) = \begin{cases} 1, & \|x_i - x_j\| \leq R_c, \\ 0, & \|x_i - x_j\| > R_c, \end{cases} \quad a_{ij} = a_{ji}, \quad a_{ii} = 0. \quad (5)$$

Here R_c is the communication radius and ε_w prevents singular weights.

With symmetric weights $w_{ij} = w_{ji} \geq 0$ and $w_{ii} = 0$, the weighted Laplacian L_w is given by

$$L_w = \operatorname{diag}\left(\sum_{j=1}^{n} w_{ij}\right) - W, \qquad W = [w_{ij}]. \quad (6)$$

Defining the stacked error vector as $\boldsymbol{\delta} = [\delta_1^\top, \ldots, \delta_n^\top]^\top$, the error dynamics can be written as

$$\dot{\boldsymbol{\delta}} = -\boldsymbol{\delta} - \Phi_\beta(\boldsymbol{\delta}) - (L_w(x) \otimes M)\boldsymbol{\delta}, \quad (7)$$

where $\Phi_\beta(\boldsymbol{\delta})$ denotes the stacked fractional-power feedback.

As the agents move, switching of the communication links introduces discontinuities in the interaction weights and the error dynamics. To establish the existence of solutions under network with switching topology, the dynamics are interpreted in the Filippov sense, $\dot{\boldsymbol{\delta}} \in \mathcal{F}[f](t, \boldsymbol{\delta})$, where f is the right-hand side of (7) and

$$\mathcal{F}[f](t, \boldsymbol{\delta}) = \bigcap_{r>0} \bigcap_{N:\,|N|=0} \overline{\operatorname{co}}\left\{f(t, z) : z \in B(\boldsymbol{\delta}, r) \setminus N\right\}.$$

Since the interaction weights are bounded, f is measurable, locally essentially bounded, and grows at most linearly. Therefore, a Filippov solution exists for every finite initial condition [17]. The coupling term can then be expressed using an effective Laplacian $\widetilde{L}_w$, which is a convex combination of the limiting weighted Laplacians. It follows that $\widetilde{L}_w^\top = \widetilde{L}_w \succeq 0$ and $\widetilde{L}_w \mathbf{1} = 0$.

Assumption 1. *Each agent obtains its own state x_i through onboard odometry and has access to its prescribed formation trajectory $x_{d,i}$ and its derivative $\dot{x}_{d,i}$. The local tracking error δ_i can therefore be computed onboard. Each agent shares its tracking error δ_i with its active neighbours through local communication, allowing it to compute the relative errors $\delta_i - \delta_j$.*

Problem statement: The research problem addressed in this paper is to develop a distributed kinematic protocol that
(i) achieves exact finite-time formation position tracking with a graph-independent settling-time bound;
(ii) establishes sufficient conditions for pairwise collision avoidance and preservation of the connected spanning subgraph $\mathcal{H}$; and
(iii) provides an offline coupling-gain selection from the planned desired formation geometry and initial disagreement.

III. Finite-Time Formation Tracking

This section establishes finite-time tracking of the prescribed formation trajectories under the proposed kinematic protocol. Explicit bounds on the tracking error and settling-time are derived along with finite-time centroid tracking.

Let $\delta_0 = \boldsymbol{\delta}(t_0)$ denote the initial formation tracking error vector. The error bound is defined as

$$\mathcal{R}(t) = \left[\left(1 + \|\delta_0\|^{1-\beta}\right)e^{-(1-\beta)(t-t_0)} - 1\right]_+^{1/(1-\beta)}, \quad (8)$$

where $[a]_+ = \max\{a, 0\}$. The finite-time arrival bound is

$$T = t_0 + \frac{\ln(1 + \|\delta_0\|^{1-\beta})}{1-\beta}. \quad (9)$$

Theorem 1 (Finite-time formation tracking)**.** *Under Assumption 1, with $M = M^\top \succeq 0$ and $0 < \beta < 1$, every Filippov solution of* (7) *satisfies*

$$\|\boldsymbol{\delta}(t)\| \leq \mathcal{R}(t), \qquad t \geq t_0 \quad (10)$$

and $\boldsymbol{\delta}(t) = 0$ for all $t \geq T$. Thus, $x_i(t) = x_{d,i}(t)$ for all agents and all $t \geq T$. The bound is independent of the interaction graph, its connectivity, and M.

Proof. Consider $V = \frac{1}{2}\|\boldsymbol{\delta}\|^2$. For almost every time, symmetry and positive semi-definiteness of the effective Laplacian and M give

$$\begin{aligned} \mathcal{D} &:= \boldsymbol{\delta}^\mathsf{T}(\widetilde{L}_w \otimes M)\boldsymbol{\delta} \\ &= \frac{1}{2}\sum_{i,j} \widetilde{w}_{ij}(\delta_i - \delta_j)^\mathsf{T} M(\delta_i - \delta_j) \geq 0. \end{aligned} \quad (11)$$

Since $1+\beta < 2$, norm monotonicity implies $\sum_{\ell=1}^{nd} |\delta_\ell|^{1+\beta} \geq \|\boldsymbol{\delta}\|_2^{1+\beta}$. Consequently along (7),

$$\dot{V} = -\|\boldsymbol{\delta}\|^2 - \boldsymbol{\delta}^\mathsf{T}\Phi_\beta(\boldsymbol{\delta}) - \boldsymbol{\delta}^\mathsf{T}(\widetilde{L}_w \otimes M)\boldsymbol{\delta} \quad (12)$$

$$\leq -\|\boldsymbol{\delta}\|^2 - \|\boldsymbol{\delta}\|^{1+\beta} = -2V - (2V)^{(1+\beta)/2}, \quad (13)$$

Let $z = \|\boldsymbol{\delta}\| = \sqrt{2V}$. Whenever $z > 0$, (13) implies $\dot{z} \leq -z - z^{\beta}$. With $y = z^{1-\beta}$,

$$\dot{y} \leq -(1-\beta)(y+1). \tag{14}$$

Integration yields $y(t)+1 \leq (y(t_0)+1)e^{-(1-\beta)(t-t_0)}$ until the tracking error reaches zero. This comparison bound establishes the bounds in (8) and (9), guaranteeing that the error reaches zero within a finite time. Since the origin is invariant under the error dynamics, the error remains zero after reaching it. Since V is non-increasing, the error remains bounded. □

A. Centroid and Formation Guarantees

Assume the formation position offsets are centered, i.e.,

$$\sum_{i=1}^{n} p_i(t) = 0, \qquad \forall t \geq t_0. \tag{15}$$

Let $c(t) = \frac{1}{n}\sum_i x_i(t)$ be the swarm centroid. Since $x_{d,i} = r + p_i$, the mean desired formation position is r.

Corollary 1 (Reference tracking)**.** *Under the centering condition* (15)*,*

$$\|c(t) - r(t)\| \leq \frac{\mathcal{R}(t)}{\sqrt{n}}, \qquad t \geq t_0. \tag{16}$$

Consequently, $c(t) = r(t)$ *for all* $t \geq T$.

Proof. Since $x_{d,i} = r + p_i$ and $\sum_{i=1}^{n} p_i = 0$, the centroid error satisfies

$$c - r = \frac{1}{n}\sum_{i=1}^{n}(x_i - x_{d,i}) = \frac{1}{n}\sum_{i=1}^{n}\delta_i.$$

By the Cauchy–Schwarz inequality,

$$\|c - r\| \leq \frac{1}{\sqrt{n}}\left(\sum_{i=1}^{n}\|\delta_i\|^2\right)^{1/2} = \frac{\|\boldsymbol{\delta}\|}{\sqrt{n}}.$$

Applying the bound $\|\boldsymbol{\delta}(t)\| \leq \mathcal{R}(t)$ from Theorem 1 gives the stated inequality. Since $\mathcal{R}(t) = 0$ for all $t \geq T$, it follows that $c(t) = r(t)$ for all $t \geq T$. □

Remark 1. *Note that when the prescribed offsets are not centered, the swarm centroid converges in finite time to* $r(t) + \frac{1}{n}\sum_{i=1}^{n} p_i(t)$*, rather than* $r(t)$*.*

IV. Disagreement-Based Safety and Connectivity Certificates

To study collision avoidance and connectivity preservation, the effect of formation tracking errors on inter-agent distances is considered. Since relative distances depend only on differences between individual tracking errors, a bound on disagreement is first derived for time-varying communication graphs. This bound is then used to establish sufficient conditions for collision avoidance and connectivity preservation. The disagreement vector is defined as

$$\begin{aligned} &\Pi = I_n - \frac{1}{n}\mathbf{1}\mathbf{1}^{\mathsf{T}}, \qquad \boldsymbol{\eta} = (\Pi \otimes I_d)\boldsymbol{\delta}, \\ &\mu = \lambda_{\min}(M) \geq 0. \end{aligned} \tag{17}$$

Thus $\eta_i = \delta_i - \bar{\delta}$ and $\delta_i - \delta_j = \eta_i - \eta_j$.

Theorem 2 (Graph-dependent disagreement contraction)**.** *For every Filippov solution at* $t \in [t_0, T]$*, the disagreement satisfies*

$$\|\boldsymbol{\eta}(t)\| \leq \|\boldsymbol{\eta}(t_0)\| \exp\left[-\int_{t_0}^{t}\left(1 + \mu\lambda_2(\widetilde{L}_w(s))\right) ds\right]. \tag{18}$$

Moreover, $\boldsymbol{\eta}(t) = 0$ *for all* $t \geq T$*. The bound remains valid across communication topology changes.*

Proof. Since $\Pi\widetilde{L}_w = \widetilde{L}_w$ and $(\Pi \otimes I_d)\boldsymbol{\eta} = \boldsymbol{\eta}$, the disagreement dynamics follow from (7) as

$$\dot{\boldsymbol{\eta}} = -\boldsymbol{\eta} - (\Pi \otimes I_d)\Phi_\beta(\boldsymbol{\delta}) - (\widetilde{L}_w \otimes M)\boldsymbol{\eta}. \tag{19}$$

For $W_\eta = \frac{1}{2}\|\boldsymbol{\eta}\|^2$, using $\boldsymbol{\eta}^{\mathsf{T}}(\Pi \otimes I_d) = \boldsymbol{\eta}^{\mathsf{T}}$ yields

$$\dot{W}_\eta = -\|\boldsymbol{\eta}\|^2 - \boldsymbol{\eta}^{\mathsf{T}}\Phi_\beta(\boldsymbol{\delta}) - \boldsymbol{\eta}^{\mathsf{T}}(\widetilde{L}_w \otimes M)\boldsymbol{\eta}. \tag{20}$$

By component-wise monotonicity of Φ_β,

$$\boldsymbol{\eta}^{\mathsf{T}}\Phi_\beta(\boldsymbol{\delta}) = \frac{1}{2n}\sum_{i,j}(\delta_i - \delta_j)^{\top}\big(\Phi_\beta(\delta_i) - \Phi_\beta(\delta_j)\big) \geq 0. \tag{21}$$

Since $M \succeq 0$ and $\mu = \lambda_{\min}(M)$, the Rayleigh quotient bound gives

$$\boldsymbol{\eta}^{\top}(\widetilde{L}_w \otimes M)\boldsymbol{\eta} \geq \mu\lambda_2(\widetilde{L}_w)\|\boldsymbol{\eta}\|^2.$$

Consequently,

$$\dot{W}_\eta \leq -2\big[1 + \mu\lambda_2(\widetilde{L}_w)\big]W_\eta.$$

Applying the comparison lemma and integrating yields (18). Finally, Π is an orthogonal projection, so $\|\boldsymbol{\eta}(t)\| \leq \|\boldsymbol{\delta}(t)\|$. By Theorem 1, $\boldsymbol{\delta}(t) = 0$ for all $t \geq T$, which implies $\boldsymbol{\eta}(t) = 0$ for all $t \geq T$. □

A. Pairwise Distance Bounds

Let $d_{ij}^q(t) = \|x_{d,i}(t) - x_{d,j}(t)\|$ and $d_{ij}^x(t) = \|x_i(t) - x_j(t)\|$.

Lemma 1 (Relative-distance envelope)**.** *For every pair* i, j*,*

$$d_{ij}^q(t) - \sqrt{2}\|\boldsymbol{\eta}(t)\| \leq d_{ij}^x(t) \leq d_{ij}^q(t) + \sqrt{2}\|\boldsymbol{\eta}(t)\|. \tag{22}$$

Proof. Since $x_i - x_j = (x_{d,i} - x_{d,j}) + (\eta_i - \eta_j)$, the triangle inequality gives

$$\|x_i - x_j\| \leq \|x_{d,i} - x_{d,j}\| + \|\eta_i - \eta_j\|,$$

while the reverse-triangle inequality yields

$$\|x_i - x_j\| \geq \|x_{d,i} - x_{d,j}\| - \|\eta_i - \eta_j\|.$$

Moreover,

$$\|\eta_i - \eta_j\| \leq \|\eta_i\| + \|\eta_j\| \leq \sqrt{2(\|\eta_i\|^2 + \|\eta_j\|^2)} \leq \sqrt{2}\|\boldsymbol{\eta}\|.$$

Hence, the two inequalities above establish the claimed bounds. □

A connected spanning sub-graph $\mathcal{H} = (\mathcal{V}, \mathcal{E}_{\mathcal{H}})$ is selected for preservation to maintain communication connectivity

throughout formation maneuvers. Let $L_{\mathcal{H}}$ denote its unweighted Laplacian. Define the maximum prescribed edge length over $\mathcal{H}$ and the minimum prescribed pairwise distance as

$$\begin{aligned} \ell_{\mathcal{H}}(t) &= \max_{(i,j)\in\mathcal{E}_{\mathcal{H}}} \|x_{d,i}(t) - x_{d,j}(t)\|, \\ d_q(t) &= \min_{i<j} \|x_{d,i}(t) - x_{d,j}(t)\|. \end{aligned} \tag{23}$$

Let $\lambda_2(L_{\mathcal{H}}) > 0$ and let $\underline{w} > 0$ be a lower bound on every active selected sub-graph-edge weight. For the range-dependent weights in (4), one may choose $\underline{w} = (R_c^{\nu} + \varepsilon_w)^{-1}$. Define

$$\begin{aligned} \gamma_{\mathcal{H}} &= 1 + \mu \underline{w} \lambda_2(L_{\mathcal{H}}), \\ \rho_0 &= \sqrt{2}\, \|\boldsymbol{\eta}(t_0)\|. \end{aligned} \tag{24}$$

Since $\boldsymbol{\eta} = (\Pi \otimes I_d)\boldsymbol{\delta}$ and Π is an orthogonal projection, it cannot increase the Euclidean norm; hence $\|\boldsymbol{\eta}(t)\| \le \|\boldsymbol{\delta}(t)\|$. By Theorem 1, this gives $\sqrt{2}\|\boldsymbol{\eta}(t)\| \le \sqrt{2}\,\mathcal{R}(t)$. Moreover, Theorem 2 gives exponential contraction of the disagreement. While all selected sub-graph edges remain active, $\widetilde{L}_w \succeq \underline{w} L_{\mathcal{H}}$, so the contraction rate is at least $\gamma_{\mathcal{H}}$. Consequently,

$$\rho_{\mathcal{H}}(t) = \min\left\{\sqrt{2}\,\mathcal{R}(t),\ \rho_0 e^{-\gamma_{\mathcal{H}}(t-t_0)}\right\}. \tag{25}$$

Thus $\rho_{\mathcal{H}}(t)$ provides an a priori bound on the maximum pairwise disagreement for every pair of agents, provided the selected sub-graph remains available.

Theorem 3 (Joint collision avoidance and connectivity preservation)**.** *If the planned formation positions satisfy, for all $t \ge t_0$,*

$$d_q(t) > d_{\text{safe}} + \rho_{\mathcal{H}}(t), \tag{26}$$

$$\ell_{\mathcal{H}}(t) < R_c - \rho_{\mathcal{H}}(t), \tag{27}$$

then every pair of agents remains strictly separated by more than d_{safe}, and all edges of the prescribed spanning sub-graph $\mathcal{H}$ remain within communication range R_c.

Proof. At t_0, (25) gives $\rho_{\mathcal{H}}(t_0) = \rho_0$, since $\|\boldsymbol{\eta}(t_0)\| \le \|\boldsymbol{\delta}(t_0)\|$. By Lemma 1 and (26), all actual pairwise distances exceed d_{safe} initially. The same lemma and (27) put all selected sub-graph links strictly inside R_c initially.

Suppose a selected sub-graph edge first reaches R_c at time $t_e > t_0$. Until t_e, all selected sub-graph edges remain active, so the lower bound $\widetilde{L}_w \succeq \underline{w} L_{\mathcal{H}}$ and Theorem 2 imply (25). By continuity, the bound also holds at t_e. For every selected sub-graph edge, Lemma 1 then gives $\|x_i(t_e) - x_j(t_e)\| \le \ell_{\mathcal{H}}(t_e) + \rho_{\mathcal{H}}(t_e) < R_c$, a contradiction. Thus the selected sub-graph persists for all time. Finally, the lower half of Lemma 1 and (26) imply $d_{ij}^x(t) > d_{\text{safe}}$ for every pair and all times. The formation position-tracking theorem is unaffected by the graph argument. □

B. Coupling-Gain Design Rule

Define the available geometric margin

$$s(t) = \min\{d_q(t) - d_{\text{safe}},\ R_c - \ell_{\mathcal{H}}(t)\}. \tag{28}$$

The margin depends only on the prescribed formation position trajectories, the selected safety threshold, the operational communication range, and the selected sub-graph. It can therefore be computed offline, before execution, without live agent-state measurements. Geometric feasibility requires $s(t) > 0$ for all $t \ge t_0$. Suppose $0 < \rho_0 < s(t_0)$. Since exact formation tracking is achieved by T, the gain need only compensate for disagreement before T. Define

$$\gamma_{\text{req}} = \sup_{t_0<t<T} \frac{\ln\left(\rho_0 / s(t)\right)}{t - t_0}. \tag{29}$$

Corollary 2 (Sufficient coupling-gain selection)**.** *A sufficient condition for Theorem 3 is*

$$1 + \lambda_{\min}(M)\, \underline{w}\, \lambda_2(L_{\mathcal{H}}) > \gamma_{\text{req}}. \tag{30}$$

For $M = mI_d$, if $\gamma_{\text{req}} > 1$, it is sufficient to choose

$$m > \frac{\gamma_{\text{req}} - 1}{\underline{w}\lambda_2(L_{\mathcal{H}})}. \tag{31}$$

Thus, once the formation position plan and physical limits (d_{safe}, R_c) are specified, the margin and required rate can be computed offline and used to select a gain satisfying the certificate.

Proof. By Theorem 3, it suffices to ensure that $\rho_{\mathcal{H}}(t) < s(t)$ throughout the maneuver. By the definition of γ_{req} in (29), $\gamma_{\mathcal{H}} > \gamma_{\text{req}}$ ensures that

$$\rho_0 e^{-\gamma_{\mathcal{H}}(t-t_0)} < s(t), \qquad t \in (t_0, T).$$

Since $\rho_{\mathcal{H}}(t) \le \rho_0 e^{-\gamma_{\mathcal{H}}(t-t_0)}$ by (25), the sufficient conditions hold on (t_0, T). The strict initial condition handles $t = t_0$. For $t \ge T$, exact formation tracking gives $\rho_{\mathcal{H}}(t) = 0 < s(t)$ by geometric feasibility. Thus, the conditions of Theorem 3 hold for all $t \ge t_0$. In particular, its minimum margin

$$\Delta_{\min} := \min_{t\in[t_0,T]} [s(t) - \rho_{\mathcal{H}}(t)] \tag{32}$$

is strictly positive, quantifying the available clearance of the certificate. □

Remark 2. *Note that when $\gamma_{\text{req}} < 1$, the conditions can be satisfied with $M = 0$, provided geometric feasibility and the initial-margin condition hold. The gain condition is sufficient but not necessary, and cannot compensate for a violation of the initial-margin condition $\rho_0 < s(t_0)$.*

V. Numerical Validation

Following the simulation setup and parameters in Table I, two sets of numerical experiments are conducted with $n = 10$ agents in $\mathbb{R}^2$: (i) finite-time formation tracking and the effect of coupling gain on convergence and control effort, and (ii) collision avoidance and connectivity preservation during rapid formation compression and expansion.

Both experiments consider a rotating star formation with angular velocity ω and time-varying scaling $a(t) = a_\infty + (a_0 - a_\infty)e^{-\kappa t}$ of the formation. The initial perturbations satisfy $\rho_0 < s(0)$. For connectivity analysis, a connected spanning sub-graph with 15 edges and $\lambda_2(L_{\mathcal{H}}) \approx 0.9316$ is selected. The simulation framework and experiments are available at this github repository.

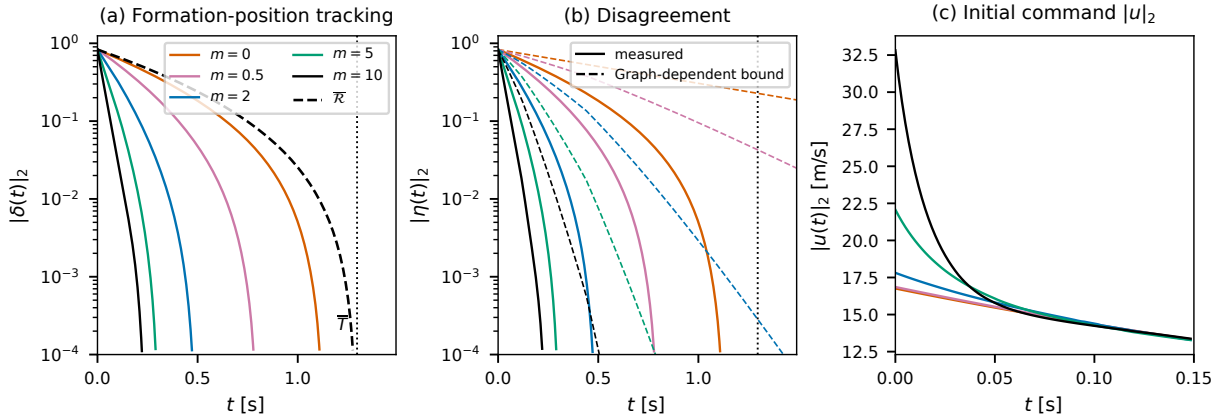


Fig. 1: Finite-time tracking, disagreement decay, and commanded-velocity magnitude across coupling gains m ($\kappa = 2.0$): (a) $\|\boldsymbol{\delta}(t)\|_2$ and theoretical bound $\overline{\mathcal{R}}(t)$ with settling-time bound T; (b) $\|\boldsymbol{\eta}(t)\|_2$ and graph-dependent bounds; (c) aggregate commanded-velocity magnitude $\|u(t)\|_2$ over the initial 0.15 s.

TABLE I: Benchmark simulation parameters.

Param.	Value	Description
n	10	Swarm size in $\mathbb{R}^2$
β	0.5	Fractional-power velocity exponent
d_{safe}	1.0 m	Minimum pairwise collision threshold
R_c	6.0 m	Maximum communication radius
ε_w	0.05	Proximity weight regularizer
ν	1	Distance exponent in interaction weights
$\underline{w}$	0.1653 m^{-1}	Uniform lower bound $1/(R_c + \varepsilon_w)$
$r(t)$	$[t,\ 2\sin(0.5t)]^{\mathsf{T}}$	Reference centroid trajectory
ω	$\pi/4$ rad/s	Star template angular rotation rate
M	mI_2	Cooperative coupling matrix ($m \geq 0$)
$\mathcal{H}$	15 edges	Five-cycle on inner agents; each outer joins two adjacent inner agents
Solver	DOP853	`rtol` $= 10^{-6}$, `atol` $= 10^{-8}$, `max_step` $= 0.02$ s

A. Finite-Time Tracking and Coupling-Gain Trade-offs

The effect of coupling gain m is evaluated during a rotating star compression ($\kappa = 2.0$, $a_0 = 1.8$, $a_\infty = 0.8$). As shown in Figure 1 and Table II, the tracking error converges within the theoretical settling-time bound $T = 1.3621$ s for all tested gains. The numerical settling time $t_{10^{-6}}$ is measured when $\|\boldsymbol{\delta}(t)\|_2$ first falls below 10^{-6}. Increasing m leads to faster tracking and disagreement convergence, while the theoretical settling-time bound remains unchanged.

To examine the associated control effort, the commanded velocity is defined as $u_i = \dot{x}_i$, with aggregate magnitude $\|u(t)\|_2 = (\sum_i \|u_i(t)\|^2)^{1/2}$. The peak commanded velocity and the integrated squared velocity $J_u = \int_{t_0}^{t_f} \|u(t)\|_2^2\, dt$ are used as measures of control effort. As shown in Table II, higher coupling gains reduce the numerical settling time but increase the commanded-velocity magnitude and overall control effort.

B. Transient Safety and Connectivity

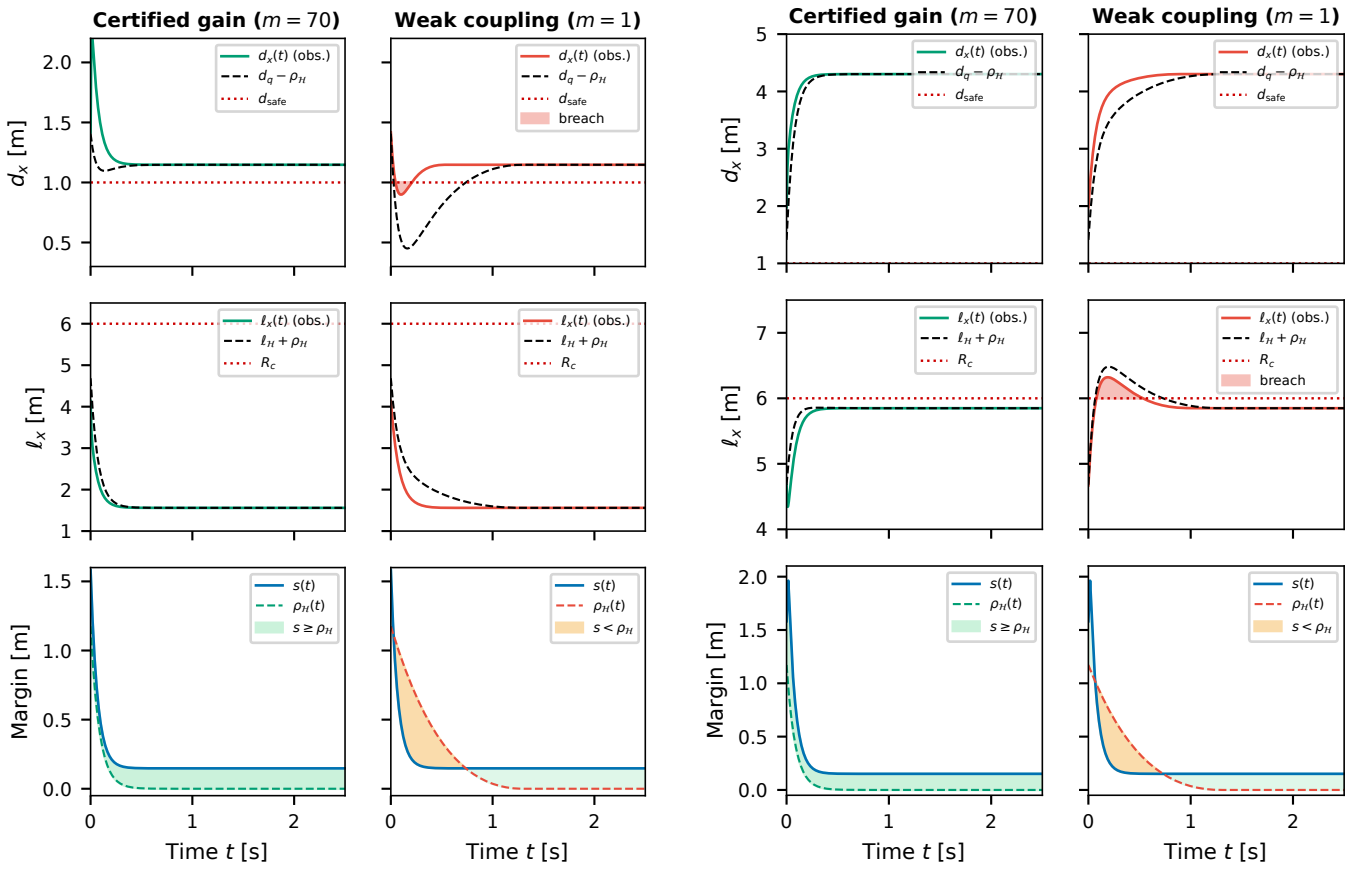
To evaluate the proposed offline gain-selection rule, we consider aggressive star compression ($a_0 = 1.80$ to $a_\infty = 0.80$) and expansion ($a_\infty = 3.00$) at $\kappa = 15.0$. As shown in Fig. 2 and Table III, the selected gain $m = 70$ satisfies the numerically evaluated safety and connectivity certificates in both maneuvers, whereas weak coupling ($m = 1$) results in collision and connectivity violations, respectively. Notably, intermediate coupling ($m = 30$) preserves both constraints despite failing the sufficient certificate, illustrating its conservatism. The reported $\Delta_{\min}$ values are estimated from sampled trajectories. Video demonstrations of the formation compression and expansion simulation experiments are available at this link.

TABLE II: Settling times and aggregate commanded-velocity metrics across coupling gains.

m	$t_{10^{-6}}$ (s)	T (s)	Peak $\|u\|_2$ [m/s]	J_u [m^2/s]
0.0	1.1517	1.3621	16.9828	429.44
0.5	0.8117	1.3621	17.0860	429.92
2.0	0.5250	1.3621	18.0322	431.55
5.0	0.4467	1.3621	22.2186	434.95
10.0	0.3933	1.3621	32.8156	440.74

VI. Conclusion

This paper developed a framework for finite-time tracking of arbitrary prescribed formation trajectories, with transient safety and connectivity certificates. Local feedback guarantees exact formation tracking within a graph-independent settling-time bound, while cooperative coupling accelerates disagreement decay without altering this guarantee. The disagreement bound yields sufficient conditions for collision avoidance and preservation of a selected connected spanning sub-graph, together with an offline coupling-gain selection rule based on planned geometric clearance and initial disagreement. Numerical experiments validate the common finite-time settling bound across coupling gains and illustrate the trade-off between faster convergence and increased control effort. Rapid formation compression and expansion illustrate how appropriately selected coupling gains can certify collision avoidance and connectivity, while insufficient coupling may lead to constraint violations. The



(a) Formation compression ($a_0 = 1.8 \to a_\infty = 0.8$).

(b) Formation expansion ($a_0 = 1.8 \to a_\infty = 3.0$).

Fig. 2: Transient safety and connectivity certificates during star compression and expansion ($\kappa = 15.0$). Columns compare certified ($m = 70$) and weak ($m = 1$) coupling; rows show the minimum pairwise distance, maximum selected-edge distance, and the geometric clearance $s(t)$ against the disagreement envelope $\rho_{\mathcal{H}}(t)$. The certificate holds when $s(t) > \rho_{\mathcal{H}}(t)$. Weak coupling leads to a collision during compression and a communication-range violation during expansion.

TABLE III: Numerically evaluated certificates and observed geometry for aggressive star maneuvers ($\kappa = 15.0$).

Maneuver	Case	m	κ	$\gamma_{\mathcal{H}}$	γ_{req}	t_{10-6} (s)	$d_{x,\min}$ (m)	$\ell_{x,\max}$ (m)	$\Delta_{\min}$ (m)	Observed outcome
Compression	Certified gain	70	15	11.7786	9.3136	0.1750	1.1473	4.1387	**0.0970**	Certified; safe, connected
	Uncertified gain	30	15	5.6194	9.3136	0.1783	1.1473	4.1387	-0.2150	Observed safe, connected
	Weak coupling	1	15	1.1540	9.3136	0.5567	0.8990	4.1387	-0.5500	Collision observed
Expansion	Certified gain	70	15	11.7786	7.4220	0.2300	1.9785	5.8490	**0.1427**	Certified; safe, connected
	Uncertified gain	30	15	5.6194	7.4220	0.4000	1.9785	5.8490	-0.1180	Safe, Observed connected
	Weak coupling	1	15	1.1540	7.4220	1.0450	1.9785	6.3214	-0.4836	Range violation observed

certificates are sufficient but not necessary, and their failure does not imply unsafe behaviour. Although the gain-selection rule provides a lower bound on coupling, actuator limits may impose practical upper bounds. Extending these guarantees to higher-order dynamics and actuator-constrained systems remains future work.

References

[1] K.-K. Oh, M.-C. Park, and H.-S. Ahn, "A survey of multi-agent formation control," *Automatica*, vol. 53, pp. 424–440, 2015.

[2] S.-J. Chung, A. A. Paranjape, P. Dames, S. Shen, and V. Kumar, "A survey on aerial swarm robotics," *IEEE Transactions on Robotics*, vol. 34, no. 4, pp. 837–855, 2018.

[3] J. A. Fax and R. M. Murray, "Information flow and cooperative control of vehicle formations," *IEEE Transactions on Automatic Control*, vol. 49, no. 9, pp. 1465–1476, 2004.

[4] B. D. O. Anderson, C. Yu, B. Fidan, and J. M. Hendrickx, "Rigid graph control architectures for autonomous formations," *IEEE Control Systems Magazine*, vol. 28, no. 6, pp. 48–63, 2008.

[5] M. Mesbahi and M. Egerstedt, *Graph Theoretic Methods in Multiagent Networks*. Princeton, NJ, USA: Princeton University Press, 2010.

[6] V. T. Haimo, "Finite time controllers," *SIAM Journal on Control and Optimization*, vol. 24, no. 4, pp. 760–770, 1986.

[7] S. P. Bhat and D. S. Bernstein, "Finite-time stability of continuous autonomous systems," *SIAM Journal on Control and Optimization*, vol. 38, no. 3, pp. 751–766, 2000.

[8] F. Xiao, L. Wang, J. Chen, and Y. Gao, "Finite-time formation control for multi-agent systems," *Automatica*, vol. 45, no. 11, pp. 2605–2611, 2009.

[9] L. Wang and F. Xiao, "Finite-time consensus problems for networks

of dynamic agents," *IEEE Transactions on Automatic Control*, vol. 55, no. 4, pp. 950–955, 2010.

[10] G. Fedele and L. D'Alfonso, "A kinematic model for swarm finite-time trajectory tracking," *IEEE Transactions on Cybernetics*, vol. 49, no. 10, pp. 3806–3815, 2019.

[11] Z. Chen, M.-C. Fan, and H.-T. Zhang, "How much control is enough for network connectivity preservation and collision avoidance?" *IEEE Transactions on Cybernetics*, vol. 45, no. 8, pp. 1647–1656, 2015.

[12] A. Filotheou, A. Nikou, and D. V. Dimarogonas, "Robust decentralised navigation of multi-agent systems with collision avoidance and connectivity maintenance using model predictive controllers," *International Journal of Control*, vol. 93, no. 6, pp. 1470–1484, 2020.

[13] J. Fu, G. Wen, X. Yu, and Z.-G. Wu, "Distributed formation navigation of constrained second-order multiagent systems with collision avoidance and connectivity maintenance," *IEEE Transactions on Cybernetics*, vol. 52, no. 4, pp. 2149–2162, 2022.

[14] Y. Huang, Z. Meng, and D. V. Dimarogonas, "Prescribed performance formation control for second-order multi-agent systems with connectivity and collision constraints," *Automatica*, vol. 160, p. 111412, 2024.

[15] R. Olfati-Saber and R. M. Murray, "Consensus problems in networks of agents with switching topology and time-delays," *IEEE Transactions on Automatic Control*, vol. 49, no. 9, pp. 1520–1533, 2004.

[16] W. Ren and R. W. Beard, "Consensus seeking in multiagent systems under dynamically changing interaction topologies," *IEEE Transactions on Automatic Control*, vol. 50, no. 5, pp. 655–661, 2005.

[17] J. Cortés, "Discontinuous dynamical systems: A tutorial on solutions, nonsmooth analysis, and stability," *IEEE Control Systems Magazine*, vol. 28, no. 3, pp. 36–73, 2008.